Study of the $^2B_1$ and $^2A_2$ States of CH_2NO_2 via Ultraviolet Photoelectron Spectroscopy of the $CH_2NO_2^-$ Anion

R. B. Metz,[†] D. R. Cyr,[‡] and D. M. Neumark*,[§]

Department of Chemistry, University of California, Berkeley, California 94720 *(Received: November 9, 1990)*

The photoelectron spectra of $CH_2NO_2^-$ and $CD_2NO_2^-$ at 355 and 266 nm have been obtained. The 355-nm spectra show extended progressions in the NO_2 symmetric stretch mode and the previously unobserved torsion mode. The experimental results have been analyzed with the aid of ab initio calculations to determine the change in geometry upon detachment of $CH_2NO_2^-$. Analysis of the spectra yields an electron affinity of 2.475 ± 0.010 eV for CH_2NO_2 and torsion barriers of 1250 cm^{-1} in CH_2NO_2 and 25 000 cm^{-1} in $CH_2NO_2^-$. This supports Jacox's conclusion that the ground state of CH_2NO_2 has a C–N single bond and indicates a C–N double bond in the anion. The 266-nm photoelectron spectrum of $CH_2NO_2^-$ has been obtained and reveals the previously unobserved $^2A_2$ electronic state of CH_2NO_2. This state lies 1.591 eV above the ground state and has a geometry similar to that of the anion.

Introduction

Negative ion photoelectron spectroscopy is a versatile technique which has been used to determine vibrational frequencies and structural information on negative ions and the neutral species formed by photodetachment.[1] It is particularly suited to the study of neutral free radicals since open-shell systems generally have positive electron affinities. The corresponding anion will therefore be stable with respect to electron detachment. However, when used alone, photoelectron spectroscopy of polyatomic anions suffers from several limitations. First, typically, only a small number of vibrational modes are active in the photoelectron spectrum; these are often (but not always) the totally symmetric modes of the neutral. Second, while the intensity distribution of the various vibrational progressions in the spectrum is directly related to the normal-mode displacements between the anion and neutral, one generally wants to convert these normal-mode displacements into changes in molecular geometry. In order to do this, it is necessary to know the form of the normal modes of vibration.[2] This requires knowing the geometry and the bond stretching and bending force constants for either the anion or the neutral. Often, neither structure is known, or not enough frequencies have been measured to determine a force constant matrix. In such cases, it is difficult to extract geometric information from the photoelectron spectrum.

Recently, Lineberger et al.[3,4] and Ellison et al.[5,6] have presented examples in which the combination of photoelectron spectroscopy and ab initio calculations provides a much more detailed picture of bonding in the anion and neutral. We have applied this combination of methods to the $CH_2NO_2^-/CH_2NO_2$ system, thereby learning about the structure and energetics of the nitromethide anion and nitromethyl radical.

The nitromethyl free radical (CH_2NO_2) is thought to be important in the thermal decomposition of nitromethane via the reaction

$$CH_3 + CH_3NO_2 \rightarrow CH_4 + CH_2NO_2 \quad \text{(ref 7)}$$

The wide use of nitromethane as a propellant, as well as its implication in reactions of the upper troposphere,[8] has provided an impetus to the recent matrix isolation[8,9] and ab initio[10,11] studies of this radical. There has been some discussion as to the structure of the nitromethyl radical. Among the structures that have been proposed[10] are planar, C_{2v} structures (**1**, **2**); planar, C_s structures (**3**), and nonplanar structures (**4**, **5**) (Chart I).

Jacox has studied the vibrational spectroscopy of the nitromethyl radical suspended in an argon matrix.[8] Thirty vibrations were found for five isotopomers. The measured frequencies were used to determine[9] a force constant matrix, based on a C_{2v} reference geometry. The excellent fit obtained shows that the ground state

CHART I

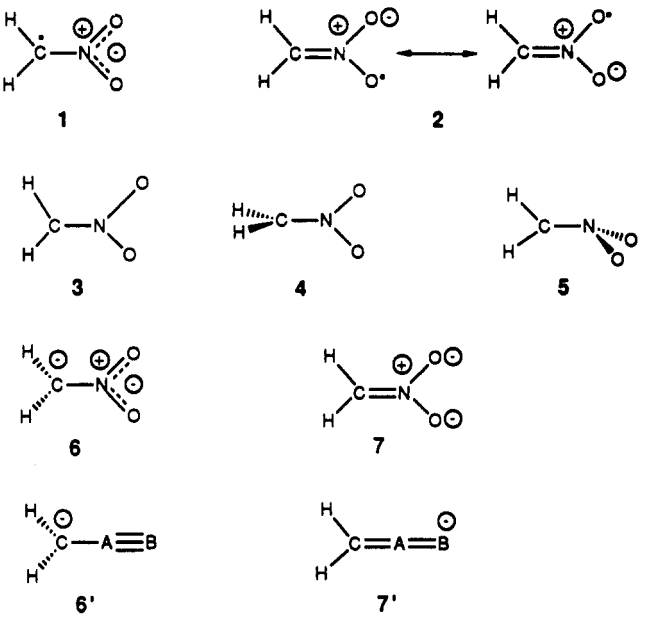

of CH_2NO_2 is planar and has C_{2v} symmetry. The force constant obtained for the C–N bond is consistent with a single bond, thus favoring structure **1** as the ground state. Ab initio calculations on nitromethyl radical have been carried out by McKee, who has

[†] University Fellow, University of California.
[‡] NSERC (Canada) Postgraduate Scholar.
[§] NSF Presidential Young Investigator and Alfred P. Sloan Fellow.

(1) Mead, R. D.; Stevens, A. E.; Lineberger, W. C. In *Gas Phase Ion Chemistry*; *Vol. 3* (*Ions and Light*); Bowers, M. T., Ed.; Academic: Orlando, FL, 1984; pp 213–248.
(2) Wilson, Jr., E. B.; Decius, J. C.; Cross, P. C. *Molecular Vibrations*; Dover: New York, 1980.
(3) Murray, K. K.; Miller, T. M.; Leopold, D. G.; Lineberger, W. C. *J. Chem. Phys.* **1986**, *84*, 2520. Christoffel, K. M.; Bittman, J. S.; Bowman, J. M. *Chem. Phys. Lett.* **1987**, *133*, 525.
(4) Ervin, K. M.; Ho, J.; Lineberger, W. C. *J. Chem. Phys.* **1989**, *91*, 5974.
(5) Moran, S.; Ellis, Jr., H. B.; DeFrees, D. J.; McLean, A. D.; Ellison, G. B. *J. Am. Chem. Soc.* **1987**, *109*, 5996.
(6) Oakes, J. M.; Harding, L. B.; Ellison, G. B. *J. Chem. Phys.* **1985**, *83*, 5400. Vazquez, G. J.; Buenker, R. J.; Peyerimhoff, S. D. *J. Chem. Phys.* **1989**, *90*, 7229.
(7) Cottrell, T. L.; Graham, T. E.; Reid, T. J. *Trans. Faraday Soc.* **1951**, *47*, 584. Nazin, G. M.; Manelis, G. B.; Dubovitskii, F. I. *Russ. Chem. Rev.* **1968**, *37*, 603. Crawforth, C. G.; Waddington, D. J. *Trans. Faraday Soc.* **1969**, *65*, 1334. Dubovitskii, F. I.; Korsunskii, B. L. *Russ. Chem. Rev.* **1981**, *50*, 958.
(8) Jacox, M. E. *J. Phys. Chem.* **1983**, *87*, 3126.
(9) Jacox, M. E. *J. Phys. Chem.* **1987**, *91*, 5038.
(10) McKee, M. L. *J. Chem. Phys.* **1984**, *81*, 3580.
(11) McKee, M. L. *J. Am. Chem. Soc.* **1985**, *107*, 1900.

0022-3654/91/2095-2900$02.50/0

studied the radical at the single[11] and multiconfiguration SCF[10] (MCSCF) levels. At the single configuration SCF level, a C_s ground state (**3**) is predicted. However, the C_{2v} ground state (**1**) is lower in energy when correlation is included (UMP2/3-21G). The MCSCF calculations favor a planar, C_s ground state (**3**), formed by a second-order Jahn–Teller interaction between the $^2B_1$ (**1**) and $^2A_2$ (**2**) states. At the highest level calculations, the predicted ground state is not yet converged with respect to the basis set used and the amount of correlation included.[10] In our discussion, we will assume a planar, C_{2v} structure for CH_2NO_2, based on the matrix isolation results.

Bonding in the nitromethide anion, $CH_2NO_2^-$, can be viewed as a competition between resonance forms **6** and **7** (Chart I). In structure **6**, the negative charge is largely localized on the carbon atom, and the C–N single bond is likely bent out of the H–C–H plane. In structure **7**, the negative charge is on the oxygen atoms, and the C–N double bond favors a planar structure. Other carbanions of the form CH_2R^- furnish examples ranging between the two extremes.[12] For example, CH_2NC^- can best be described by structure **6′**, with a C–N single bond and a C–N triple bond, rather than by structure **7′** (two C–N double bonds).[13] This gives rise to a nonplanar structure and leaves the negative charge substantially localized on the methylene group. Methylene groups are poor electron acceptors, so the electron binding energy of CH_2NC^- is quite low (1.059 eV). CH_2CN^- has substantially more contribution from structure **7′**, leading to a more nearly planar structure, as well as a higher electron binding energy[5] (1.543 eV). CH_2CHO^- goes even further, with structure **7′** dominating, leading to a planar anion with a C–C double bond and a high binding energy (1.825 eV).[14] We will show that $CH_2NO_2^-$ also has structure **7**, and an even higher binding energy (2.475 eV).

In this paper we present the photoelectron spectra of $CH_2NO_2^-$ and $CD_2NO_2^-$ and the result of ab initio calculations on $CH_2NO_2^-$ and CH_2NO_2. We will use these results to show that $CH_2NO_2^-$ is planar, with an electron affinity of 2.475 eV. We will also offer support for Jacox's assignment[9] of **1** as the ground state of CH_2NO_2 from a measurement of the (infrared inactive) torsion vibration. In addition, we will present experimental results on an excited electronic state of CH_2NO_2 corresponding to structure **2**.

Experimental Section

The photoelectron spectrometer used in this work has been described previously,[15] so only a brief description will be presented. Negative ions are generated by crossing a pulsed molecular beam with a 1-keV electron beam. Ions cool in the supersonic expansion; negative ions are extracted from the beam, accelerated to 1 keV, and mass-separated by using a Wiley-McLaren time-of-flight mass spectrometer.[16] The mass-selected ion of interest is intersected by the third (355 nm, 3.495 eV) or fourth (266 nm, 4.660 eV) harmonic of a pulsed Nd:YAG laser. A small fraction (0.01%) of the detached electrons are detected at the end of a 1-m field-free region perpendicular to the ion and laser beams. Photoelectron flight times are then converted to energy. The resolution of the spectrometer is 8 meV (64 cm^{-1}) at 0.65 eV electron kinetic energy (eKE) and degrades as $(eKE)^{3/2}$ at higher eKE. The eKE of a given anion → neutral transition is

$$eKE = h\nu - EA + E^{(-)} - E^{(0)}$$

where EA is the electron affinity, $E^{(-)}$ is the internal energy of the negative ion and $E^{(0)}$ is the internal energy of the neutral. Peaks at *higher* eKE correspond to transitions to states of the radical with *lower* internal energy.

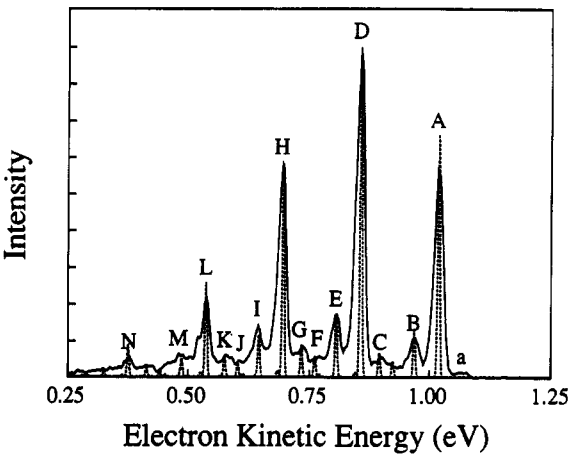

Figure 1. Experimental (—) and simulated (- - -) 355-nm photoelectron spectra of $CH_2NO_2^-$. The simulated spectrum has been convoluted with 5-meV Gaussians, for comparison with experiment. The experimental peaks are ~20 meV wide.

TABLE I: Peak Positions[a] in the 355-nm Photoelectron Spectrum of $CH_2NO_2^-$ (a) and $CD_2NO_2^-$ (b)

(a) $CH_2NO_2^-$

peak	ν_3	ν_4	ν_6	eKE, eV
a				1.07
A	0	0	0	1.020
B	0	0	2	0.969
C	0	1	0	0.902
D	1	0	0	0.858
E	1	0	2	0.808
F	1	0	4	0.774
G	1	1	0	0.738
H	2	0	0	0.696
I	2	0	2	0.646
J	2	0	4	0.607
K	2	1	0	0.579
L	3	0	0	0.537
M	3	0	2	0.485
N	4	0	0	0.375

(b) $CD_2NO_2^-$

peak	ν_2	ν_4	ν_6	eKE, eV
a				1.053
A	0	0	0	1.015
B	0	0	2	0.982
C	0	0	4	0.935
D	0	1	0	0.899
E	1	0	0	0.853
F	1	0	2	0.818
G	1	0	4	0.782
H	1	1	0	0.729
I	2	0	0	0.692
J	2	0	2	0.657
K	2	1	0	0.578
L	3	0	0	0.532
M	3	0	2	0.496
N	4	0	0	0.374

[a] The average uncertainty in peak positions is 0.007 eV.

Nitromethide ions are generated by passing 1 atm of NF_3 over CH_3NO_2 at room temperature and expanding the mixture through a pulsed molecular beam valve. The likely mechanism for $CH_2NO_2^-$ formation is as follows. First, dissociative attachment of low-energy secondary electrons from the 1-keV electron beam produces F^-:

$$NF_3 + e^- \rightarrow NF_2 + F^-$$

Fluoride ion then reacts with nitromethane entrained in the beam to produce nitromethide by proton abstraction:

$$CH_3NO_2 + F^- \rightarrow CH_2NO_2^- + HF$$

(12) Pross, A.; DeFrees, D. J.; Levi, B. A.; Pollack, S. K.; Radom, L.; Hehre, W. J. *J. Org. Chem.* **1981**, *46*, 1693.
(13) Moran, S.; Ellis, Jr., H. B.; DeFrees, D. J.; McLean, A. D.; Paulson, S. E.; Ellison, G. B. *J. Am. Chem. Soc.* **1987**, *109*, 6004.
(14) Mead, R. D.; Lykke, K. R.; Lineberger, W. C.; Marks, J.; Brauman, J. I. *J. Chem. Phys.* **1984**, *81*, 4883.
(15) Metz, R. B.; Weaver, A.; Bradforth, S. E.; Kitsopoulos, T. N.; Neumark, D. N. *J. Phys. Chem.* **1990**, *94*, 1377.
(16) Wiley, W. C.; McLaren, I. H. *Rev. Sci. Instrum.* **1955**, *26*, 1150.

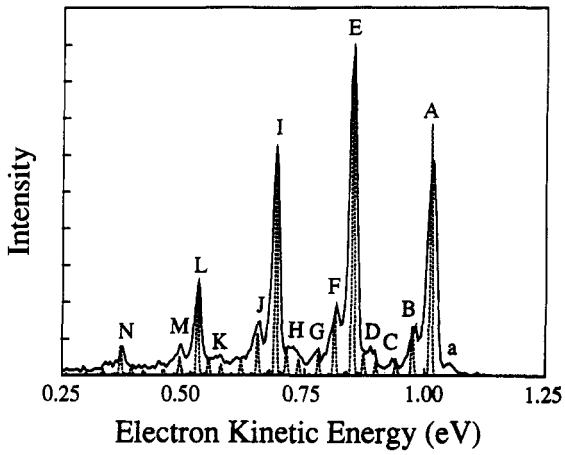

Figure 2. Experimental (—) and simulated (---) 355-nm photoelectron spectra of $CD_2NO_2^-$. The simulated spectrum has been convoluted with 5-meV Gaussians, for comparison with experiment. The experimental peaks are ~20 meV wide.

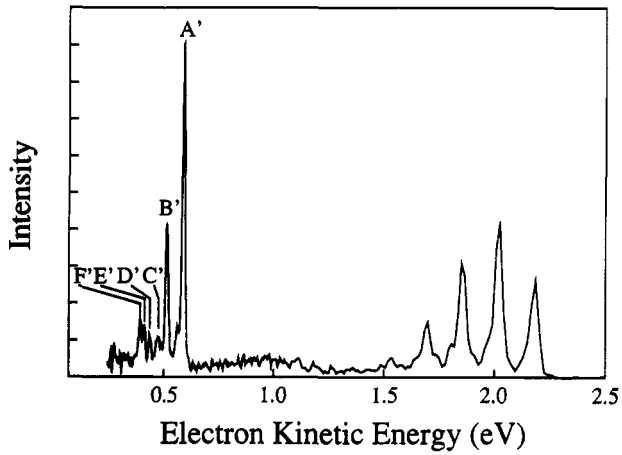

Figure 3. The 266-nm photoelectron spectrum of $CH_2NO_2^-$.

The photoelectron spectra shown were obtained by averaging over 150000 laser shots. All spectra were taken with the laser polarized perpendicular to the direction of electron collection.

Results

The 355-nm photoelectron spectra of $CH_2NO_2^-$ and $CD_2NO_2^-$ are shown in Figures 1 and 2. The positions of the features in each spectrum are given in Table I. The spectra are surprisingly simple, considering that nitromethide possesses 12 vibrational modes. Peak A, at 1.020 eV, is identified as the 0–0 band, giving a raw electron affinity of 2.475 ± 0.010 eV. Peak a (the small feature at 1.07 eV) is a "hot band" due to detachment of vibrationally excited ions. The remaining features in the spectrum are believed to originate from the ground vibrational state of the ion.

The prominence of a single progression in the $CH_2NO_2^-$ spectrum (peaks A, D, H, L, N) indicates that most of the geometry change between ion and neutral is along a single normal mode. The peaks in this progression are spaced by 0.161 eV (1300 ± 25 cm^{-1}). The photoelectron spectrum of $CD_2NO_2^-$ (Figure 2) shows a similar progression (peaks A, E, I, L, N) with a nearly identical spacing of 1292 ± 25 cm^{-1}. Two smaller progressions are also evident. The first (A–B, D–E–F, H–I–J, L–M) is at 409 cm^{-1} in the $CH_2NO_2^-$ spectrum and shifts to 280 cm^{-1} (A–B–C, E–F–G, I–J, L–M) in the $CD_2NO_2^-$ spectrum, indicating that this mode involves hydrogen atom motion. There is also a less intense progression (A–C, D–G, H–K) at 954 ± 25 cm^{-1} in the $CH_2NO_2^-$ spectrum. A similar, but less resolved, progression (A–D, E–H, I–K) appears in the $CD_2NO_2^-$ spectrum.

The 266-nm photoelectron spectrum of $CH_2NO_2^-$ (Figure 3) shows a series of peaks at high electron kinetic energy due to detachment to the ground electronic state of CH_2NO_2, as well as sharp peaks at low eKE due to an excited electronic state of CH_2NO_2 lying 1.591 eV above the ground state (Table II). This excited-state spectrum is less extended than the ground-state spectrum, suggesting that the excited state has a geometry more similar to the anion. In addition, there is a small, very broad feature at ~1.0 eV electron kinetic energy, between the two sharp bands. The intensity of this band lies just above the noise level in the spectrum. The 266-nm photoelectron spectrum of $CD_2NO_2^-$ is very similar to that of $CH_2NO_2^-$. The 355-nm spectrum will be discussed first; the excited-state results at 266 nm will be briefly discussed at the end of the paper.

TABLE II: Peak Positions[a] in the 266-nm Photoelectron Spectrum of $CH_2NO_2^-$

peak	eKE, eV	assignment	peak	eKE, eV	assignment
A′	0.594	0^0	D′	0.443	5^2
B′	0.519	5^1	E′	0.415	3^1
C′	0.478	(4^1)	F′	0.396	

[a] The average uncertainty in peak positions is 0.007 eV.

TABLE III: Vibrational Frequencies of CH_2NO_2

mode	sym	matrix freq, cm^{-1}	description
1	a_1	3055	CH_2 sym stretch
2	a_1	1419	CH_2 scissors
3	a_1	1297	NO_2 sym stretch
4	a_1	986	CN stretch
5	a_1	693	NO_2 scissors
6	a_2	*a*	torsion
7	b_1	719	CNO_2 out-of-plane
8	b_1	606	H_2CN out-of-plane
9	b_2	3200	CH_2 antisym stretch
10	b_2	(1484, 1461)[b]	NO_2 antisym stretch
11	b_2	1095	CH_2 rock
12	b_2	(484)[c]	NO_2 rock

[a] This mode is not infrared active and was not seen in the matrix studies. [b] In Fermi resonance with ($\nu_4 + \nu_{12}$). [c] Estimated from the position of ($\nu_4 + \nu_{12}$) peak. All values are from the matrix studies of refs 8 and 9.

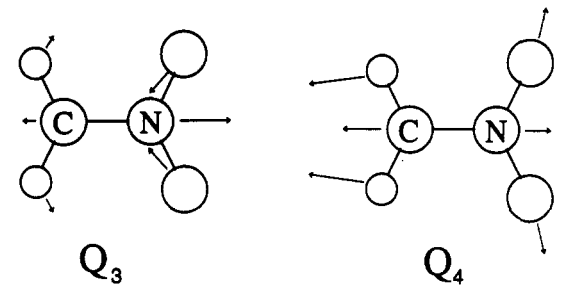

Figure 4. Form of Q_3 (NO_2 symmetric stretch) and Q_4 (C–N stretch) normal modes of the CH_2NO_2 radical.

Analysis and Discussion

1. Qualitative Features. If the ion and neutral have the same symmetry, transitions from the vibrational ground state of the anion to vibrations of any quanta in totally symmetric (a_1, assuming C_{2v} symmetry) modes and vibrations of *even* quanta in non totally symmetric modes are allowed.[17] The intensity of the allowed peaks is governed by the Franck–Condon principle. Because of this, the frequency of a nonsymmetric mode must be substantially different in the neutral and anion before the vibration will be active and the photoelectron spectrum is typically dominated by progressions in totally symmetric modes.

The peaks in the main progression in the $CH_2NO_2^-$ spectrum are spaced by 1300 cm^{-1}. A comparison with the matrix isolation frequencies of CH_2NO_2 (Table III) shows that this is a progression in the NO_2 symmetric stretch (ν_3, a_1 symmetry), found at 1297 cm^{-1} in the matrix studies.[8] The form of this normal mode is

(17) Eland, J. H. D. *Photoelectron Spectroscopy*; Butterworth and Co.: London, 1984.

TABLE IV: Ab Initio Results on $CH_2NO_2^-$ and CH_2NO_2

R_{CH}, Å	R_{CN}, Å	R_{NO}, Å	∠HCN, deg	∠CNO, deg	energy (+240 h)	level	ref
			$CH_2NO_2^-$ ($\tilde{X}$, $^1A_1$)				
1.066	1.295	1.346	118.7	119.7	−1.663 32	HF/3-21G	20
1.066	1.290	1.315	118.6	120.4	−2.69278	HF/4-31G	12
1.071	1.313	1.255	118.1	120.3	−3.05770	HF/6-31G*	21
1.069	1.308	1.258	117.8	120.4	−3.08915	HF/6-31^{++}G**	this work
1.074	1.347	1.292	117.4	120.1	−3.80446	MP2/6-31^{++}G**	this work
			CH_2NO_2 ($\tilde{X}$, $^2B_1$)				
1.065	1.408	1.257	116.6	117.1	−1.62566	UHF/3-21G	11
1.077	1.470	1.291	116.3	116.5	−2.09675	UMP2/3-21G	11
1.067	1.418	1.198	116.5	117.1	−3.02981	UHF/6-31G	11
1.073	1.430	1.243	116.4	117.1	−3.72090	UMP2/6-31^{++}G**	this work
			CH_2NO_2 (Twisted, ϕ = 90°, $^2B_2$)				
1.068	1.449	1.191	116.5	117.0	−3.71262	UMP2/6-31^{++}G**	this work
			CH_2NO_2 ($^2A_2$)				
1.072	1.318	1.313	117.2	123.7	−3.62282	UMP2/6-31^{++}G**	this work

shown in Figure 4. The C–N bond lengthens as the N–O bonds shorten and the O–N–O angle increases.

The remaining peaks in the spectrum can be identified as combination bands superimposed on the main progression. The small peaks (C, G, K) which appear 0.118 eV (954 ± 25 cm^{-1}) from the ν_3 peaks are assigned to the C–N stretch (ν_4), found at 986 cm^{-1} in the matrix studies. This totally symmetric mode (Figure 4) is complementary to the ν_3 mode; as the C–N bond stretches, the N–O bonds lengthen and the O–N–O angle increases.

The medium-sized peaks (B, E, I, M) at 0.051 eV (409 cm^{-1}) and the smaller features 0.087 eV (700 cm^{-1}) from the main peaks in the spectrum of $CH_2NO_2^-$ are somewhat more puzzling. The lowest frequency vibration observed in the matrix studies is the NO_2 rock (ν_{12}) at 484 cm^{-1}. If the anion and neutral are both planar, C_{2v} species, we would only observe even quanta of this (nontotally symmetric) mode, leading to a spacing of 968 cm^{-1}. The lowest totally symmetric vibration is the ν_5 (NO_2 scissors) mode at 693 cm^{-1}. The frequency of the mode we observe shifts to 280 cm^{-1} in the spectrum of $CD_2NO_2^-$. Both ν_5 and ν_{12} were found to have much smaller H–D isotope shifts in the matrix studies. Thus, none of the vibrations observed in the matrix studies appears to be responsible for the 409-cm^{-1} peaks. There is one vibrational mode in the ion that is not infrared active: the torsion mode (ν_6). This is a nontotally symmetric mode with a_2 symmetry. The torsion mode primarily involves hydrogen atom motion, leading to a large frequency shift upon deuteration. We will show that the torsion mode is responsible for this progression. We believe that, for CH_2NO_2 (CD_2NO_2), two quanta of this mode are at 409 (280) cm^{-1}, and four quanta are near 700 (~600) cm^{-1}.

It is somewhat surprising that a progression in a nontotally symmetric vibration is observed in the photoelectron spectrum. The reason that the usual propensity rule is not followed will be examined with the aid of molecular orbital theory and ab initio calculations which show that the ν_6 frequency is very different in the anion and neutral. In addition, the calculations show the changes in structure and bonding expected upon photodetachment.

2. Molecular Orbital Picture. Simple molecular orbital arguments can be used to gain a qualitative feel for the bonding in nitromethyl radical. To construct the molecular orbitals for CH_2NO_2 and $CH_2NO_2^-$, we use the procedure described by Walsh[18] and treat the CH_2 group as a single atom with six valence electrons. Both the anion and radical are assumed to be planar and to have C_{2v} symmetry. The relative energies of the molecular orbitals are based on orbital energies found in our ab initio calculation on $CH_2NO_2^-$. The highest occupied molecular orbitals for $CH_2NO_2^-$ have the electron configuration $[8a_1^2\ 5b_2^2\ 1a_2^2\ 2b_1^2]$. The highest occupied molecular orbital ($2b_1$) is C–N π-bonding, N–O antibonding, and weakly O–O bonding (Figure 5a). Removal of an electron from the $2b_1$ orbital, which results in the $^2B_1$ ground state of CH_2NO_2, would cause the C–N bond to lengthen (as the double bond becomes a single bond), the N–O bond to shorten, and the O–N–O angle to increase. These changes in geometry should lead to excitation of the ν_3 mode upon detachment, the primary feature observed in the spectrum. In addition, the torsion potential for the $^2B_1$ state should be very different from that of the anion. Twisting about the single bond in the $^2B_1$ state should involve only a small barrier, while twisting about the double bond in the anion should have a very large barrier.

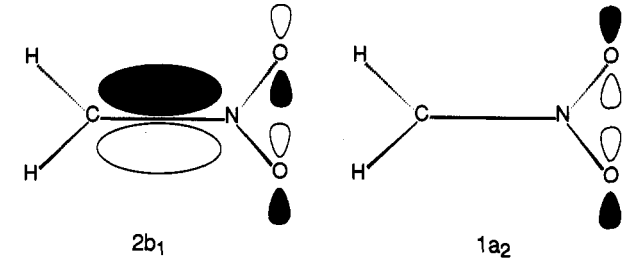

Figure 5. Highest occupied molecular orbitals of the $CH_2NO_2^-$ anion. The $2b_1$ orbital (a, left) is C–N π bonding, N–O π antibonding, and O–O π bonding. The $1a_2$ orbital (b, right) is weakly O–O π antibonding. Removal of an electron from the $2b_1$ orbital of the anion forms the $^2B_1$ ground state of the CH_2NO_2 radical; removal of an electron from the $2a_1$ orbital forms the low-lying $^2A_2$ excited state of CH_2NO_2.

The next highest molecular orbital in the ion is the $1a_2$, which consists of out-of-plane π orbitals on the oxygens (Figure 5b). This orbital is weakly O–O antibonding, but is basically nonbonding, so the $^2A_2$ state of the radical is expected to have a geometry similar to the anion. Note that this implies that the $^2A_2$ state has a C–N double bond (structure **2**), whereas the $^2B_1$ state has a C–N single bond (structure **1**).

3. Ab Initio Calculations. To gain a more quantitative picture than that afforded by simple MO theory, ab initio calculations on CH_2NO_2 and $CH_2NO_2^-$ were performed using the GAUSSIAN 88 package.[19] Although several authors have reported calculations on $CH_2NO_2^-$,[12,20,21] the highest level calculations were carried out at the uncorrelated SCF level by Edgecombe and Boyd[21] using the 6-31G* basis set (polarization functions on heavy atoms only). It is well-known[22] that diffuse functions are very useful in describing the delocalized extra electron in anions, and it is essential to include correlation effects, if one is to predict electron affinities.[22] We have therefore optimized the geometry of $CH_2NO_2^-$ (within

(18) Walsh, A. D. *J. Chem. Soc.* **1953**, 2260.

(19) Frisch, M. J.; Head-Gordon, M.; Schlegel, H. B.; Raghavachari, K.; Binkley, J. S.; Gonzalez, C.; DeFrees, D. J.; Fox, D. J.; Whiteside, R. A.; Seeger, R.; Melius, C. F.; Baker, J.; Martin, R. L.; Kahn, L. R.; Stewart, J. J. P.; Fluder, E. M.; Topiol, S.; Pople, J. A. Gaussian Inc., Pittsburgh, PA.

(20) Bigot, B.; Roux, D.; Salem, L. *J. Am. Chem. Soc.* **1981**, *103*, 5271. Ritchie, J. P. *J. Am. Chem. Soc.* **1985**, *107*, 1829.

(21) Edgecombe, K. E.; Boyd, R. J. *Can J. Chem.* **1983**, *61*, 45.

(22) Baker, J.; Nobes, R. H.; Radom, L. *J. Comput. Chem.* **1986**, *7*, 349.

TABLE V: Ab Initio Vibrational Frequencies of $CH_2NO_2^-$ at HF/6-31^{++}G**

mode	sym	freq,[a] cm^{-1}	description[b]
1	a_1	3019	CH_2 sym stretch
2	a_1	1452	CH_2 scissors
3	a_1	1349	NO_2 sym stretch
4	a_1	1014	CN stretch
5	a_1	646	NO_2 scissors
6	a_2	637	torsion
7	b_1	785	CNO_2 out-of-plane
8	b_1	535	H_2CN out-of-plane
9	b_2	3131	CH_2 antisym stretch
10	b_2	1357	NO_2 antisym stretch
11	b_2	1054	CH_2 rock
12	b_2	542	NO_2 rock

[a] The ab initio frequencies have been scaled by 0.9. [b] The description of the modes is only approximate and has been done by analogy with CH_2NO_2.

the C_{2v} point group) at the HF/6-31^{++}G** (polarization and diffuse functions on all atoms) and MP2/6-31^{++}G** levels (correlation included via second-order Moller–Plesset perturbation theory). Our results are compared to earlier results in Table IV. We have also tried allowing the anion to become nonplanar (while maintaining C_s symmetry), but a planar geometry is preferred. Planar, C_s geometries were not explored. Anion geometries significantly distorted from C_{2v} (especially in-plane distortions) would be expected to lead to the excitation of b_2 modes in the radical. This is not observed in the photoelectron spectrum. The planar structure is in contrast to the barrier to planarity seen in CH_2NC^-,[13] so structure **6** contributes little. Frequencies for $CH_2NO_2^-$ were calculated at the HF/6-31G^{++}G** level (Table V). All the frequencies are real, so the C_{2v} structure is at least a local minimum. The lowest frequency in the ion is the out-of-plane distortion (ν_8) at 535 cm^{-1}. All Hartree–Fock frequencies have been scaled[23] by 0.9.

McKee has done a great deal of ab initio work on the CH_2NO_2 radical.[10,11] A C_{2v} ground state (**1**) is predicted at the single configuration SCF (UMP2/3-21G) level.[11] He has also performed multiconfiguration SCF (MCSCF) calculations.[10] In the MCSCF calculations, the geometry was first optimized by using a single configuration, at both C_s and C_{2v} symmetry. MCSCF energies were then determined at these geometries. The MCSCF calculations predict a planar, C_s ground state (**3**), although the predicted geometry is sensitive to basis set and degree of correlation. In addition, McKee calculated SCF frequencies using several basis sets, including 6-31G*.

On the basis of the matrix spectroscopy work,[9] which indicates a C_{2v} geometry for CH_2NO_2, we calculated optimized C_{2v} geometries at the UHF/6-31^{++}G** and UMP2/6-31^{++}G** levels. Our results are shown and compared to McKee's in Table IV. We also investigated small distortions from planarity (still retaining C_s symmetry). At the UHF/3-21G level, a slightly nonplanar geometry is favored, but at the UHF/6-31^{++}G** level a planar geometry is preferred. The electron affinity of CH_2NO_2 is predicted to be 2.274 eV at the UMP2/6-31^{++}G** level, in reasonable agreement with the experimental value of 2.475 eV. Calculations at the MP2 level using basis sets that include diffuse functions have been found to give surprisingly accurate molecular electron affinities.[22]

The torsion was explored by calculating energies with the CH_2 group perpendicular to the NO_2 group ($\phi = 90°$, Figure 6). All other bond lengths and angles were left at the planar minimum. Results are summarized in Table VI. For $CH_2NO_2^-$, the torsion barrier is 20724 cm^{-1} (UHF/6-31^{++}G**) and 16620 cm^{-1} (UMP2/6-31^{++}G**). This barrier is characteristic of a C–N double bond; for comparison, the torsion barrier in ethylene is 22750 cm^{-1},[24] as twisting the molecule breaks the π-bonding,

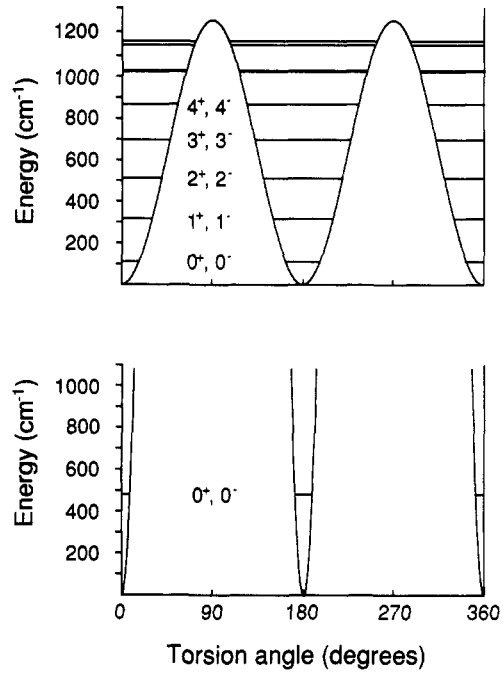

Figure 6. Torsion potentials and energy levels for CH_2NO_2 (top) and $CH_2NO_2^-$ (bottom). The torsion angle ϕ is the angle between the NO_2 and CH_2 planes. It is 0° for the planar configuration, 90° at the twisted geometry, and 180° at the second (equivalent) planar configuration.

TABLE VI: Torsion Barriers for $CH_2NO_2^-$ and CH_2NO_2[a]

barrier, cm^{-1}	method	ref
	$CH_2NO_2^-$ ($\tilde{X}$, $^1A_1$)	
20724	HF/6-31^{++}G**//MP2/6-31^{++}G**	this work
16620	MP2/6-31^{++}G**	this work
25000	fit to peak intensities	this work
	CH_2NO_2 ($\tilde{X}$, $^2B_1$)	
3452	UHF/3-21G	this work
2649	UMP2/3-21G	this work
2833	UHF/6-31G//UHF/3-21G	10
1504	UMP2/6-31G//UHF/3-21G	10
2343	UMP3/6-31G//UHF/3-21G	10
1859	UMP2/6-31^{++}G**	this work
1817	UMP2/6-31^{++}G**†	this work
1250	fit to peak positions	this work
	CH_2NO_2 ($^2A_2$)	
31020	UHF/6-31G//UHF/3-21G	10
30740	UMP2/6-31G//UHF/3-21G	10
30110	UMP3/6-31G//UHF/3-21G	10

[a] The torsion barrier was calculated as the difference in energy between the molecule at the optimized C_{2v} geometry with the torsion angle $\phi = 0°$ and 90°. The geometry was not reoptimized at $\phi = 90°$, except for the one identified by † and values from ref 10.

reducing the double bond to a single bond. The torsion barrier is much lower for CH_2NO_2. It is 3095 cm^{-1} at the UHF/6-31^{++}G** level and 1859 cm^{-1} at the UMP2/6-31^{++}G** level. For comparison, the torsion barrier about the single bond in ethane is 960 cm^{-1}.[25] Allowing the other bond lengths to change in the twisted geometry (within the C_{2v} framework) lowered the torsion barrier by only 42 cm^{-1}, to 1817 cm^{-1}. The torsion barrier is very sensitive to the amount of C–N π bonding in the molecule, much more so than the C–N stretching force constant. The small barrier strongly suggests that the C–N bond is a single bond, and, although resonance structures for the radical can be drawn with both C–N single (**1**) and double bonds (**2**), only the single-bonded structure

(23) Pople, J. A.; Schlegel, H. B.; Krishnan, R.; DeFrees, D. J.; Binkley, J. S.; Frisch, M. J.; Whiteside, R. A.; Hout, R. F., Jr.; Herhe, W. J. *Int. J. Quantum Chem., Quantum Chem. Symp.* **1981**, *15*, 269. DeFrees, D. J.; McLean, A. D. *J. Chem. Phys.* **1985**, *82*, 333.

(24) Hollas, J. M. *High Resolution Spectroscopy*; Butterworth and Co.: London, 1982; p 263.

(25) Herzberg, G. *Infrared and Raman Spectra*; Van Nostrand Rheinhold Co.: New York, 1945.

TABLE VII: Geometry Change on $CH_2NO_2^-$ Detachment

R_{CH}, Å	R_{CN}, Å	R_{NO}, Å	∠HCN, deg	∠CNO, deg	method
−0.001	0.083	−0.049	−1.0	−3.0	ab initio MP2/6-31^{++}G**
0.002	0.085	−0.047	−0.9	−3.0	experiment
	(0.009)	(0.006)	(0.1)	(0.2)	uncertainty

contributes significantly for the ground state of the radical. McKee[10] reports similar results for the torsion barrier in the $^2B_1$ ground state and a torsion barrier of about 30 000 cm^{-1} in the $^2A_2$ state of the radical, consistent with structure **2**.

Our calculations of the anion and neutral geometries at the MP2/6-31^{++}G** level allow us to predict geometry changes upon detachment. Changes in the CH_2 group are predicted to be small (Table VII). The C–H bonds lengthen by 0.001 Å, and the H–C–H angle increases by 2.0°, which is consistent with the lack of high-frequency vibrations in the spectrum. Upon detachment, the C–N double bond in the anion becomes a single bond, and the N–O bonds become stronger. The C–N bond lengthens significantly by 0.083 Å, the N–O bonds shorten by 0.049 Å, and the O–N–O angle increases by 5.9°. These geometry changes are consistent with excitation of the NO_2 stretching mode (ν_3) (Figure 4), which lengthens the C–N bond, while shortening the N–O bond and widening the O–N–O angle. The change in the C–N bond leads to a dramatic change in the torsion barrier, and this is manifested in the spectrum as an excitation of the torsion (ν_6) mode.

4. Detailed Analysis of Spectrum. In this section, we use the experimental spectra and some of the ab initio results to quantitatively determine structural and bonding changes upon photodetachment. These can then be compared to the changes predicted purely on the basis of the ab initio calculations. The torsion potential, which is very sensitive to the nature of the C–N bond, will be treated first. The symmetric modes, including a prediction of the geometry change upon photodetachment based on our experimental results, will be treated in the next section.

(*a*) *Torsion.* The torsion is the only vibration of a_2 symmetry and can thus be treated separately from the other 11 modes. The Hamiltonian for this system is[26]

$$\mathcal{H} = -\frac{\hbar^2}{2I}\frac{\partial^2}{\partial\phi^2} + V(\phi) \tag{1}$$

where ϕ is the torsion angle (the angle between the CH_2 and NO_2 planes). I is the reduced moment of inertia for the system

$$I = \frac{I_{CH_2}I_{NO_2}}{I_{CH_2} + I_{NO_2}} \tag{2}$$

where

$$I_{CH_2} = 2M_H[R_{CH}\sin(\angle HCN)]^2 \tag{3}$$

$$I_{NO_2} = 2M_O[R_{NO}\sin(\angle CNO)]^2 \tag{4}$$

Using the UMP2/6-31^{++}G** geometry, $I_{CH_2} = 1.861$ amu·Å^2, $I_{CD_2} = 3.719$ amu·Å^2, and $I_{NO_2} = 39.152$ amu·Å^2, so I is 1.777 amu·Å^2 for both CH_2NO_2 and $CH_2NO_2^-$ and 3.396 amu·Å^2 for CD_2NO_2 and $CD_2NO_2^-$. We use a potential[25] of the form

$$V(\phi) = (b/2)[1 - \cos(2\phi)] \tag{5}$$

where b is the torsion barrier. This is a double minimum potential, with minima at $\phi = 0°$ and 180°, where ϕ is 0° for the planar configuration, 90° at the twisted geometry, and 180° for the second (equivalent) planar configuration.

If $b = 0$, then $V(\phi) = 0$ and the solutions[26] to the Schrodinger equation are the free-rotor wave functions $P_j^0(\phi)$ with energy

$$E_j^0 = j^2\hbar^2/2I \tag{6}$$

For $b \neq 0$, we expand the wave function in a free-rotor basis

$$P_v(\phi) = \sum_{j=-N}^{N} C_{j,v}P_j^0(\phi) \tag{7}$$

Matrix elements of the Hamiltonian can be found analytically and are given by

$$H_{j,k} = \langle P_j^0|\mathcal{H}|P_k^0\rangle = \left(E_j^0 + \frac{b}{2}\right)\delta_{j,k} - \frac{b}{4}\delta_{j+2,k} - \frac{b}{4}\delta_{j,k+2} \tag{8}$$

The (tridiagonal) Hamiltonian matrix is set up using a basis of 71 free-rotor functions ($N = 35$) and diagonalized by using standard routines. Franck–Condon factors are given by

$$\mathrm{FCF} = |\langle P'_v|P''_v\rangle|^2 = [\sum_{j=1}^{N} C''_{j,v''}C'_{j,v'}]^2 \tag{9}$$

where the primed quantities refer to the neutral wave function and the doubly primed to the anion.

The experimental peak spacings and intensities are best fit with $b' = 1250 \pm 250$ cm^{-1} in the radical and $b'' = 25\,000 \pm 10\,000$ cm^{-1} in the anion. The corresponding potentials are shown in Figure 6, along with several low-lying vibrational levels. The lowest anion levels are far below the barrier. For these levels, the potential looks much like that for two distinct harmonic oscillators, one with a minimum at $\phi = 0°$, the other at 180°. Eigenvalues occur in pairs. For $CH_2NO_2^-$, the first two are at 485 cm^{-1} and are separated by $\ll$0.01 cm^{-1}. These correspond to two $v = 0$ harmonic oscillator wave functions: in phase (forming the 0^+ wave function) and out of phase (forming the 0^- wave function). These nearly degenerate levels are equally populated in our ion beam. The next pair of levels ($1^+/1^-$) are 964 cm^{-1} higher in energy and are not expected to be populated in our ion beam. Similarly, for the neutral, using $b' = 1250$ cm^{-1}, the first few levels occur in nearly degenerate pairs. The $0^+/0^-$ peaks lie 106 cm^{-1} above the minimum, the $1^+/1^-$ peaks are 208 cm^{-1} above the $0^+/0^-$, the $2^+/2^-$ are 405 cm^{-1} above the $0^+/0^-$, etc. From the 0^+ level of the anion, only transitions to the 0^+, 2^+, 4^+, ... levels of the neutral are allowed by symmetry.[27] From the 0^- level, transitions to the 0^-, 2^-, 4^-, ... levels are allowed. As both the 0^+ and 0^- levels are equally populated in our source, the peaks in our spectrum are due to transitions from the $0^+/0^-$ states of the ion to the $0^+/0^-$, $2^+/2^-$, and $4^+/4^-$ levels of the neutral. Note that the 4^+ and 4^- states are separated by only 0.35 cm^{-1}, which is far below our resolution, and the separation between the lower lying pairs is even smaller.

The peak positions are quite sensitive to b', while the peak intensities are not very sensitive to b'', so the value obtained for b'' must be considered approximate. The values from the analysis of the spectrum are in fairly good agreement with our best ab initio values ($b' = 1817$ cm^{-1}, $b'' = 16\,600$ cm^{-1}; Table VI). A progression in the nontotally symmetric torsion mode occurs because the torsion potentials for the ion and neutral are very different. The torsion "frequency" (the 0^+ to 1^+ spacing) is 964 cm^{-1} in the anion and 208 cm^{-1} in the radical, although they both have minima at $\phi = 0°$ and 180° corresponding to a planar, C_{2v} structure.

The value of b'' is consistent with a C–N double bond in the anion, and b' is consistent with a C–N single bond in the ground state of the radical. This change in bonding is supported by the C–N stretching force constant, which drops from a scaled, ab initio value of 7.59×10^2 N/m in the $CH_2NO_2^-$ anion to 4.89×10^2 N/m in the CH_2NO_2 radical. In spite of this change in the C–N bond, the frequency of the CN stretch mode changes very little upon detachment (it is 1014 cm^{-1} in $CH_2NO_2^-$ and 986 cm^{-1} in CH_2NO_2). This is because the CN stretch mode involves a significant amount of N–O stretching, and the N–O bonds strengthen when the C–N bond weakens. The C–N bond length also changes upon detachment. This will be examined in the next section.

(*b*) *Totally Symmetric Modes.* The remaining progressions in the spectrum are due to the totally symmetric ν_3 and ν_4 vi-

(26) Atkins, P. W. *Molecular Quantum Mechanics*; Oxford University Press: Oxford, U.K., 1983; pp 58–63.

(27) Herzberg, G. *Electronic Spectra of Polyatomic Molecules*; Van Nostrand Reinhold Co.: New York, 1966; p 152.

TABLE VIII: Force Constants for CH_2NO_2[a]

force const	old value	uncertainty	new value	uncertainty
CH	5.34	0.01	5.34	0.01
CN	4.75	0.20	4.89	0.22
NO	8.07	0.32	8.51	0.32
HCH	0.28	0.01	0.27	0.01
HCN	0.70	0.01	0.70	0.01
ONO	1.79	0.18	1.89	0.22
CNO	1.07	0.14	0.96	0.04
NO, NO	2.24	0.39	1.64	0.42
NO, CN	1.15	0.29	1.37	0.26
NO, HCN	−0.10	0.06	−0.01	0.05
NO, ONO	0.29	0.17	0.20	0.16
NO, CNO	−0.28	0.26	0.33	0.32
CN, HCH	−0.27	0.02	−0.27	0.02
CN, ONO	−0.49	0.07	−0.68	0.09
HCN, CNO	0.09	0.02	0.08	0.03
HCN, ONO	−0.06	0.03	−0.03	0.04

[a] Stretching and stretching interaction force constants are in 10^2 N/m; bending and bending interaction force constants are in 10^{-18} N·m; stretch–bending interaction force constants are in 10^{-8} N. Old values are from ref 9 and use a reference geometry with ∠HCH = 122° and ∠ONO = 122°. New values use our UMP2/6-31++G** reference geometry, with ∠HCH = 127.2° and ∠ONO = 125.8°. The fit is insensitive to bond lengths. All values are fit to the 30 frequencies given in ref 8.

brations of the radical. The corresponding Q_3 and Q_4 normal modes are shown in Figure 4. The normal-mode displacements upon detachment can be determined by fitting the observed peak intensities for these progressions. We assume the two modes are separable and have the same form in the anion as in the neutral. This parallel mode approximation[28] is justified by the nearly equal ν_3 and ν_4 experimental neutral and ab initio ion frequencies. The best fit to the spectrum is given by a displacement of 0.26 (±0.03) Å·amu$^{-1/2}$ in Q_3 and 0.08 (±0.02) Å·amu$^{-1/2}$ in Q_4, where the uncertainties include the effect of varying the anion frequency by ±20%. The simulated spectrum is shown in Figure 1 (dotted lines). The simulated spectrum includes progressions in the ν_3, ν_4, and ν_6 modes and shows good agreement with experiment. The simulated peaks have been given widths of 5 meV to facilitate comparison with experiment. The actual peaks observed are ~20 meV wide.

In order to relate these normal-mode displacements to changes in internal coordinates, we need the form of the normal modes.[2] The force constant matrix (and hence the normal modes) were determined by Jacox[9] by fitting 30 matrix frequencies for five isotopomers of CH_2NO_2. This was done by using a particular reference geometry for CH_2NO_2; we have repeated the calculation using our best ab initio reference geometry. The results of the fit (including the form of the normal modes) do not depend on the bond lengths but are slightly sensitive to changes in bond angles.[9] The reference geometry used by Jacox had C_{2v} symmetry with ∠HCH = 122° and ∠ONO = 122°, compared to our best ab initio values of 127.2° and 125.8°. Thus, we have fit the 30 matrix frequencies to the same 16 parameter force constant matrix used by Jacox, using our MP2 reference geometry. The fit (Table VIII) is slightly better than that obtained by Jacox, the average difference between predicted and observed frequencies in our fit is 1.8 cm^{-1}, versus 2.2 cm^{-1}. The C–H stretching force constant (F_{CH}) is unchanged, F_{CN} increases from 475 to 489 N/m (still consistent with a C–N single bond), and F_{NO} increases from 807 and 851 N/m. The fitted force constants (using the MP2 reference geometry) and corresponding normal modes are used in the remainder of the analysis. As mentioned above, the neutral modes are used for the anion. We can now use the photoelectron spectrum to determine the change in molecular geometry upon detachment.

For harmonic modes (as we have here), the photoelectron spectrum gives the geometry change, but not the direction in which it occurs. Here we first turn to the molecular orbital arguments for qualitative insight. Photodetachment to the $^2B_1$ ground state removes an electron from the $2b_1$ orbital, which is C–N π-bonding and N–O antibonding. We therefore expect the C–N bond to lengthen and the N–O bond to shorten, so the direction of the Q_3 displacement between the anion and neutral is that shown in Figure 4. The lengthening of the C–N bond should weaken it, and this is also consistent with the large drop in the torsion barrier. The Q_4 mode also chiefly involves C–N stretching, but the displacement in this mode is smaller than the Q_3 displacement. One can infer the sign of the displacement in Q_4 from the ab initio calculations, which predict that the C–N bond lengthens by 0.083 Å upon detachment (Table VII). The Q_3 displacement accounts for 0.063 Å. If we add the change in C–N bond length due to ν_4 (0.022 Å), then the C–N bond is predicted to lengthen by 0.085 Å; if we substract it we get only 0.041 Å. Adding it is clearly in better agreement with the ab initio results, so the Q_4 displacement is also as shown in Figure 4. The experimentally predicted and ab initio geometry change upon detachment are in excellent agreement (see Table VII). The photoelectron spectrum does not directly give the geometry of either the ion or neutral; it gives the change in geometry between the two. Unfortunately, there is no experimental geometry available for either species. If the geometry of the ion or neutral were accurately known, our experimental results would give the geometry of the other species.

Once the geometry change for $CH_2NO_2^-$ detachment has been determined and the force constant matrix is known, we can simulate the photoelectron spectrum of $CD_2NO_2^-$. This provides a check on our fit. The result is shown in Figure 2. The simulated spectrum is also in excellent agreement with experiment. The peaks in the photoelectron spectra of $CH_2NO_2^-$ and $CD_2NO_2^-$ are about 15 meV broader than our instrumental resolution. This may be due to the presence of sequence bands (transitions from $v'' = 1$ in the anion to $v' = 1$ in the neutral).

Thus far, we have assumed that all the features we observe are due to CH_2NO_2. Several studies[29-31] have shown that CH_3NO_2 can isomerize to methyl nitrite, CH_3ONO, which lies 0.1 eV higher in energy, by passing over a 2.4-eV barrier.[29] Presumably, nitrite isomers also exist for CH_2NO_2 and $CH_2NO_2^-$. These isomers are not likely to be responsible for the structure in our spectra. If the $CH_2NO_2 \rightarrow CH_2ONO$ isomerization barrier is similar to that of CH_3NO_2, photodetachment of $CH_2NO_2^-$ would access states of CH_2NO_2, while detachment of CH_2ONO^- would access states of CH_2ONO. The anions in our source are formed by the reaction

$$F^- + CH_3NO_2 \rightarrow HF + CH_2NO_2^-$$

which is 0.6 eV exothermic. Even if the entire exothermicity were left in the $CH_2NO_2^-$, this is not likely to be enough energy to surmount the isomerization barrier and form CH_2ONO^-. The observed ground-state frequencies are in excellent agreement with those of CH_2NO_2, so the dominant isomer in the beam is clearly $CH_2NO_2^-$. If the CH_2ONO^- isomer were present in the beam, it would be expected to have a lower electron affinity than $CH_2NO_2^-$ and thus contribute features at higher electron kinetic energy than peak A. Using methyl nitrite as a precursor could well lead to formation of the CH_2ONO^- anion

$$F^- + CH_3ONO \rightarrow HF + CH_2ONO^-$$

The photoelectron spectrum of CH_2ONO^- would then give information on the potential energy surface near the CH_2ONO minimum.

5. Excited Electronic State. The 266-nm photoelectron spectrum of $CH_2NO_2^-$ (Figure 3) shows structure due to an excited electronic state of the CH_2NO_2 radical. The progression due to

(28) Ervin, K. M.; Ho, J.; Lineberger, W. C. *J. Phys. Chem.* **1988**, *92*, 5405.

(29) Wodtke, A. M.; Hintsa, E. J.; Yee, Y. T. *J. Phys. Chem.* **1986**, *90*, 3549.

(30) Wodtke, A. M.; Hintsa, E. J.; Lee, Y. T. *J. Chem. Phys.* **1986**, *84*, 1044.

(31) Dewar, M. J. S.; Ritchie, J. P.; Alster, J. *J. Org. Chem.* **1985**, *50*, 1031.

this electronic state is significantly less extended than that due to the ground state, suggesting that this electronic state looks more like the anion than the ground state does. This state is likely formed by the removal of a slightly O–O antibonding $1a_2$ electron from the anion, forming the $^2A_2$ excited state. This state is predicted to lie 0.35 eV *below* the $^2B_1$ ground state in McKee's MCSCF + CI calculations[10] and 2.67 eV *above* the ground state in our single configuration (MP2/6-31^{++}G**) calculations. Experimentally, it lies 1.591 eV *above* the $^2B_1$ state.

The analysis of the photoelectron spectrum of the excited state is somewhat more complicated than that of the ground state, due to the lack of previous experimental information on the $^2A_2$ state. Ab initio calculations on the excited state are difficult, because it is an excited state of a radical and suffers from significant spin contamination.[22,32] We have calculated the geometry of the $^2A_2$ state at the UMP2/6-31^{++}G** level (Table IV). This result is expected to be less accurate than the results on $CH_2NO_2^-$ and CH_2NO_2 ($^2B_1$). The removal of a nonbonding electron from $CH_2NO_2^-$ is expected to have little effect on the force constants—the vibrational frequencies of the $^2A_2$ state are expected to be close to those of the anion, so rather than calculate frequencies for the $^2A_2$ state, we have used the frequencies calculated for $CH_2NO_2^-$ (Table V). Peak A′ (0.594 eV, Table II) is clearly the origin. Peak B′ (605 cm^{-1} from the origin) is assigned to one quanta in the ν_5 (NO_2 scissors) mode (646 cm^{-1} in the anion). Peak D′ (1218 cm^{-1}) corresponds to two quanta in ν_5. The observed excitation of the NO_2 scissors mode is reasonable, as the most significant geometry change upon detachment to the $^2A_2$ state is a 7.2° decrease in the O–N–O angle, consistent with removing an electron from an O–O antibonding orbital.

The remaining small peaks are likely due to a small excitation in the other totally symmetric modes. Thus, peak C′ (936 cm^{-1}) could correspond to ν_4 (CN stretch, 1014 cm^{-1} in the ion) and peak E′ (1444 cm^{-1}) could be due to one quanta in the ν_3 (NO_2 symmetric stretch) mode (1349 cm^{-1} in the ion). It is not clear what peak F′ is due to. The photoelectron spectrum of the $^2A_2$ state is basically unchanged by deuteration. No progression in the torsion is expected (or seen), as both the anion and $^2A_2$ state have large calculated barriers to torsion (20 000–30 000 cm^{-1}).[10]

The broad feature at ~1.0-eV electron kinetic energy in Figure 3 could be due to an unresolved extended progression spread over many vibrational modes. This may result from transitions to an electronic state with a geometry significantly distorted from C_{2v}. Thus, this broad feature may be an observation of a state of CH_2NO_2 corresponding to structure **3**, **4**, or **5**. Also, our results do not preclude the possibility that there are other excited states of CH_2NO_2 below the $^2A_2$ state. Only states formed by removing one electron from the anion will be seen in the photoelectron spectrum[1] (i.e., we would not see quartet states, as these would involve removing one electron and promoting one electron). Thus, while the $^2A_2$ state is certainly a low-lying excited electronic state of CH_2NO_2, it is not necessarily the lowest excited state.

6. Thermodynamics. The electron affinity of the nitromethyl radical can be used to derive several thermodynamic quantities. The C–H bond strength in nitromethane can be determined from[33]

$$D(\text{H–CH}_2\text{NO}_2) = \Delta_{\text{H,acid}}(\text{CH}_3\text{NO}_2) + \text{EA}(\text{CH}_2\text{NO}_2) - \text{IP(H)}$$

where $\Delta_{\text{H,acid}}(CH_3NO_2)$ is the gas-phase acidity of nitromethane (1493 ± 12 kJ/mol).[34] The electron affinity of CH_2NO_2 is 239 ± 1 kJ/mol and the ionization potential of hydrogen is 1312 kJ/mol. This gives a bond dissociation energy of 420 ± 12 kJ/mol. This value, with the heat of formation of nitromethane (−75 ± 1 kJ/mol)[33] gives a value of 127 ± 12 kJ/mol for the heat of formation of CH_2NO_2. If we assume the electron to have a heat capacity of zero, then the heat of formation of $CH_2NO_2^-$ is approximately

$$\Delta_f H(\text{CH}_2\text{NO}_2^-) = \Delta_f H(\text{CH}_2\text{NO}_2) - \text{EA}(\text{CH}_2\text{NO}_2)$$

This gives $\Delta_f H(CH_2NO_2^-) = -112 \pm 12$ kJ/mol, in excellent agreement with the previous value (−114 ± 13 kJ/mol).[33]

Conclusion

From the photoelectron spectra of $CH_2NO_2^-$ and $CD_2NO_2^-$ we find an electron affinity of 2.475 ± 0.010 eV for CH_2NO_2 (2.480 ± 0.010 eV for CD_2NO_2). Our results are consistent with a planar, C_{2v} anion with a large (25 000 cm^{-1}) torsion barrier, indicative of a C–N double bond. The planar geometry and high electron affinity suggest that structure **7** is the dominant resonance contribution in $CH_2NO_2^-$. The major geometry change on detachment of an electron from $CH_2NO_2^-$ is the change of a C–N double bond to a single bond, evidenced by a lengthening of the C–N bond and a large drop in the torsion barrier (to 1250 cm^{-1}) in CH_2NO_2. This supports Jacox's assignment[9] of structure **1** with a C–N single bond as the ground ($^2B_1$) state of CH_2NO_2. The geometry change upon detachment determined from the photoelectron spectrum is in excellent agreement with our ab initio prediction (Table VII). We have also observed the excited ($^2A_2$) state 1.591 eV above the ground state. The $^2A_2$ state has structure **2** with a C–N double bond, giving it a geometry similar to that of $CH_2NO_2^-$.

Acknowledgment. Support from the National Science Foundation under contract no. CHE-8803729 is gratefully acknowledged. We thank the San Diego Supercomputer Center for a grant to undertake the ab initio calculations. We thank Alex Weaver for her help in conducting the experiments.

Registry No. CH_2NO_2, 16787-85-2; $CH_2NO_2^-$, 18137-96-7.

(32) Gill, P. M. W.; Radom, L. *Chem. Phys. Lett.* **1986**, *132*, 16.

(33) Lias, S. G.; Bartmess, J. E.; Liebman, J. F.; Holmes, J. L.; Levin, R. D.; Mallard, W. G. *J. Phys. Chem. Ref. Data* **1988**, *17*, 1 (Suppl. 1).

(34) Bartmess, J. E.; Scott, J. A.; McIver, Jr., R. T. *J. Am. Chem. Soc.* **1979**, *101*, 6047. Cumming, J. B.; Kebarle, P. *Can. J. Chem.* **1978**, *56*, 1.